Received: 20 May 2022 | Revised: 24 August 2022 | Accepted: 25 August 2022

DOI: 10.1111/cas.15563

ORIGINAL ARTICLE

Cancer Science WILEY

Suppression of high mobility group box 1 in B16F10 tumor does not inhibit the induction of neoantigen-specific T cells

Kayoko Waki | Miyako Ozawa | Akira Yamada

Cancer Vaccine Development Division, Research Center for Innovative Cancer Therapy, Kurume University, Kurume, Fukuoka, Japan

Correspondence
Akira Yamada, Cancer Vaccine Development Division, Research Center for Innovative Cancer Therapy, Kurume University, Kurume, Fukuoka 830-0011, Japan.
Email: akiymd@med.kurume-u.ac.jp

Funding information
Japan Society for the Promotion of Science, Grant/Award Number: JP19K07742

Abstract

Accumulated clinical data of immune checkpoint blockades have suggested the importance of neoantigens in cancer immunity. Tumor antigens are released from dead cancer cells together with cellular components, such as damage-associated molecular patterns (DAMPs), into the tumor microenvironment. We recently reported that high mobility group box 1 (HMGB1), a representative DAMP molecule, showed a negative impact on anti-tumor immunity. However, a positive role of HMGB1 in the initiation of innate and subsequent adaptive immunity has also been demonstrated; thus, the effects of HMGB1 on anti-tumor immunity have not been well understood. In this study, we identified nine immunogenic neoantigen epitopes of B16F10 murine melanoma cells and subsequently investigated the effects of suppression of HMGB1 on the induction of neoantigen-specific immunity using HMGB1-knockout tumors. Neoantigen-reactive T cells were expanded in B16F10 tumor-bearing mice, and T cell receptor repertoire analysis suggested that neoantigen-reactive T cells were oligoclonally increased in B16F10 tumor bearers. An increase of neoantigen-reactive T cells and oligoclonal expansion of the T cells were similarly detected in HMGB1-knockout tumor-bearing mice. The induction of neoantigen-specific immunity under the suppression of HMGB1 in the tumor microenvironment shown in this study supports further development of combination therapy of HMGB1 suppression with neoantigen-targeted cancer immunotherapies, including immune checkpoint blockade therapy.

KEYWORDS
alarmin, cytotoxic T-lymphocytes, HMGB1, neoantigen, tumor microenvironment

1 | INTRODUCTION

Cancer immunotherapy, particularly immune checkpoint blockade (ICB) therapy, has become a major modality of cancer treatment for various cancers. Accumulated clinical data suggest that cancers with a high tumor mutation burden (TMB) are more effective targets of ICB therapy.[1–4] Nonsynonymous mutation in cancer cells generates neoantigens; thus, cancers with a high TMB have a greater number of neoantigens than low-TMB cancers.[2,4] These findings also suggest the importance of neoantigen-induced immunity in ICB therapy.[2,5] The clinical efficacy of ICB monotherapy is limited, and combination therapies of ICBs with other therapeutic modalities are currently under

development.[6–8] Cancer vaccine therapy is one of the promising modalities of combination therapy. We previously developed a personalized peptide vaccine, in which three or four peptides are selected for vaccination from a peptide panel consisting of 31 CTL-epitope peptides according to the patient's HLA-A locus type and pre-existing immunity.[9–11] During the past two decades, we have conducted several clinical trials of personalized peptide vaccine therapy in patients with various advanced cancers.[9–11] Vaccine therapy has shown clinical benefits in some patients; however, the effect is limited, similarly to that of ICB monotherapy.[10,11] Like most cancer vaccines developed by other groups, our cancer vaccine used non-mutated tumor antigens.[9–13] However, after the discovery of the importance of neoantigen-reactive immunity in ICB therapy, the trend in cancer vaccines has been to switch from non-mutated antigens to neoantigens in the hopes of surpassing the equivocal success of existing vaccines.[14–18]

Tumor antigens are released to the tumor microenvironment (TME) from dead cancer cells, together with cellular components, such as damage-associated molecular patterns (DAMPs), also called alarmins.[19,20] The effects of tumor-derived DAMPs on anti-tumor immunity have not been well understood. We recently reported that high mobility group box 1 (HMGB1), a representative DAMP molecule, showed a negative impact on anti-tumor immunity.[21] Namely, knockout (KO) of HMGB1 in the tumor cells using CRIPR/Cas9 suppressed in vivo tumor growth mediated by host CD8 T cells and accelerated infiltration of T cells as well as macrophages and dendritic cells (DCs) into the tumor tissues.[21] Our previous study[22] as well as others[23–25] regarding the anti-tumor effect of HMGB1 inhibitors, suggested a possible application of suppression of tumor-derived HMGB1 to cancer immunotherapy, such as ICB and neoantigen vaccine therapies.[21–25] Although most previous studies supported the negative effect of HMGB1 on anti-tumor immunity,[21–25] a positive role of HMGB1 in the initiation of innate and subsequent adaptive immunity has also been shown.[26,27] Namely, the binding of HMGB1 to receptors, such as Toll-like receptor (TLR)-2, TLR-4, and the receptor for advanced glycation end products (RAGE), on macrophages and dendritic cells induces proinflammatory cytokines through activation of interferon regulatory factor-3 (IRF3) and subsequently triggers innate immunity.[27,28] Therefore, it is still unclear whether the suppression of HMGB1 in the TME would affect the induction of anti-tumor immunity.

In this study, we identified immunogenic neoantigens of B16F10 murine melanoma cells and subsequently investigated the effect of the suppression of HMGB1 on the induction of neoantigen-specific immunity using HMGB1-KO tumors.

2 | MATERIALS AND METHODS

2.1 | Mice

Seven-week-old female C57BL/6J (B6) mice were purchased from CLEA Japan (Tokyo, Japan) and housed under specific pathogen-free conditions in the animal facility of Kurume University School of Medicine. All animal experimental protocols were approved by the Institutional Animal Care and Use Committee of Kurume University (approval no. 2019-030) in accordance with the national guidelines on the care and use of laboratory animals. In the tumor transplantation experiments, tumor size was measured every 2 or 3 days. Humane endpoints in this study were as follows: (1) tumor size reached >20 mm in diameter, (2) lethargic condition, and (3) 60 days after tumor transplantation. To obtain tumor tissues or lymphoid tissues, the mice were euthanized by cervical dislocation. Experimental groups and the number of mice in each group were as follows: in vivo immunogenicity analysis consisted of 50 mutated and control Trp2 peptide groups ($n = 3$) for the first screening and 10 mutated, 10 wild-type (WT), and control Trp2 peptide groups ($n = 3$) for the second screening; neoepitope reactive T cell analysis consisted of WT, G9, and A10E2 tumor-bearer groups ($n = 3$) at days 9 and 14 of tumor transplantation; T cell receptor (TcR) repertoire analysis of neoantigen immunized mice consisted of nine mutated and control Trp2 peptide groups ($n = 3$); TcR repertoire analysis of tumor-bearing mice consisted of WT, G9, and A10E2 tumor groups ($n = 3$).

2.2 | Cells

Murine melanoma B16F10 cells were purchased from the American Type Culture Collection (ATCC) through Summit Pharmaceuticals. The cells were cultured in high glucose D-MEM (Fujifilm Wako Pure Chemical, Osaka, Japan) supplemented with 10% FCS (Thermo Fisher, Waltham, MA), L-glutamine, and 50 μg/ml gentamicin at 37°C in a 5% CO_2 incubator. The B16F10-derived HMGB1-KO clones (G9 and A10E2) were previously established in our laboratory.[21] The linear donor was inserted around cDNA position 198 in exon 2 of the HMGB1 gene, which was 25 nucleotides downstream of the initiation codon, and all the functional domains of HMGB1 were disrupted in these KO clones. The KO cells from frozen stock were used within 1 month of in vitro culture after thawing. Under this condition, no expression of HMGB1 was confirmed.

2.3 | Whole-exosome sequencing and RNA-Seq

Genomic DNA and RNA samples of B16F10 cells were prepared using NucleoSpin Blood (TaKaRa Bio, Kusatsu, Japan) and TRIzol (ThermoFisher), respectively, according to the manufacturer's instructions. Whole-exosome sequencing and RNA-Seq were performed by the Kazusa DNA Research Institute using HiSeq 1500 (Illumina). A total of 848 gene mutations, including 566 nonsynonymous mutations, were detected.

2.4 | Prediction of MHC class-I binding and peptide synthesis

Potential peptides containing the nonsynonymous mutations in the sequences that would bind to H-2K^b or H-2D^b were predicted using

the Immune Epitope Database (IEDB) MHC-I binding predictions with the NetMHCpan algorithm.[29] We obtained 602 peptide sequences, both of 9-mer and 10-mer, that seemed to have potential for H-2K^b or H-2D^b binding. After excluding sequences expected to be difficult to synthesize and solubilize, we selected the top 50 sequences with high affinity to H-2K^b or H-2D^b (IC50 < 283 nM) and had the peptides synthesized by GenScript (Piscataway, NJ). The purity of the peptides was ≥70%. Each peptide was dissolved in dimethyl sulfoxide (Fujifilm Wako Pure Chemical) at a concentration of 10 mg/ml and stored at −80°C. Just before use, the peptide stock solution was diluted to a concentration of 0.5 mg/ml with PBS and used as a working solution. Tyrosinase-related protein 2 (Trp2), a melanocyte differentiation antigen expressed in B16 melanoma cells, TRP2-derived H-2K^b-restricted peptide (SVYDFFVWL)[30] was purchased from MBL and used as a positive control.

2.5 | In vivo immunogenicity of neoantigens

Each peptide was solubilized in dimethyl sulfoxide and diluted by PBS. A total of 0.2 ml of 50 μg peptide with 50 μg of poly (I:C; InvivoGen; San Diego, CA) was subcutaneously (s.c.) injected into the tail base of C57BL/6 mice (n = 3) on days 0 and 7. Mice were killed on day 14, and the spleens were obtained. In vivo immunogenicity was assessed by IFN-γ enzyme-linked immunospot (ELISPOT) assay for individual mice; 5×10^5 of spleen cells from immunized mice were mixed with 5×10^4 of bone marrow-derived DCs and cultured in the presence or absence of 2 μg/ml peptide for 18 h in wells of a 96-well MutliScreen HA plate (Millipore) coated with 10 μg/ml of anti-mouse IFN-γ mAb (AN18, Mabtech, Nacka Strand, Sweden) with X-vivo 15 (Lonza) and supplemented with 2 mM L-glutamine, 10 mM HEPES and 50 μg/ml gentamicin at 37°C in a 5% CO_2 incubator. After washing away the cells, the plate was incubated with 1 μg/ml of biotinylated anti-mouse IFN-γ Ab (R4-6A2, Mabtech) for 2 h at room temperature (rt), followed by 1 h incubation of 1:1000-diluted ExtrAvidin-alkaline phosphatase (Sigma-Aldrich) at rt. IFN-γ-producing cell spots were visualized using a SIGMAFAST BCIP/NBT tablet (Sigma-Aldrich) and counted using an ImmunoSpot Analyzer (Cellular Technology). DCs were prepared according to the previous reports.[31] In brief, bone marrow cells from C57BL6 mice were suspended in 10% FCS-RPMI1640 medium (Nacalai Tesque, Kyoto, Japan) supplemented with 50 μM 2-mercaptoethanol, 20 ng/ml GM-CSF (PeproTech, Cranbury, NJ) and 20 ng/ml IL-4 (PeproTech) at a density of 2.5×10^5 cells/ml, and 12 ml of the cell suspension was placed into a T75 flask and cultured at 37°C in a 5% CO_2 incubator. On day 3, an additional 12 ml of medium was added to the flask, and on day 6, the cells were harvested, resuspended in 12 ml of fresh medium and returned to the original flask. On day 9, the cells were harvested and stored in an LN_2 tank. The quality of the DC preparations was as follows: CD11c$^+$ 78.7% (95%CI 73.1–84.1), I-A$^+$ 50.3% (95%CI 42.7–57.8), CD11b$^+$ 67.1% (95%CI 61.0–73.2), CD86$^+$ 32.1% (95%CI 27.4–36.9), and CD40$^+$ 40.1% (95%CI 35.9–44.4). One day before use, the cells were thawed, washed, and cultured with 20 ng/ml IL-4 at 37°C.

2.6 | T-cell receptor repertoire analysis

RNA samples of day 14 spleen cells from mice (n = 3) immunized on days 0 and 7 with each neoantigen peptide or Trp2 peptide (50 μg) with 50 μg of poly (I:C) were prepared using RNeasy Plus Universal Mini Kit (QIAGEN) according to the manufacturer's instructions and subjected to TcR repertoire analysis. From tumor-bearing mice (n = 3), the spleens and tumor tissues were harvested on day 14. For tumor-infiltrated lymphocytes (TIL) isolation, 1- to 2-mm^3 blocks of tumor tissue were cultured in individual wells of a 24-well plate with 2 ml RPMI (Nacalai Tesque) supplemented with 10% FCS, 25 mM HEPES, 2 mM L-glutamine, 50 μM 2-mercaptoethanol, 50 μg/ml gentamicin, and 6000 units/ml IL-2 (Imunace 35, Shionogi, Osaka, Japan). On day 7, half the culture medium was replaced with fresh medium and TILs were harvested on day 8. RNA samples of day 14 spleen cells and TILs were prepared using NucleoSpin RNA Plus (TaKaRa Bio) according to the manufacturer's instructions and subjected to TcR repertoire analysis. Genes encoding the complementarity-determining region 3 (CDR3) of TcR-β were analyzed by Takara Bio or Repertoire Genesis (Ibaraki, Japan) using a SMARTer Mouse TcR α/β Profiling Kit (Clontech) with a MiSeq next-generation sequencer (Illumina).

2.7 | Neoepitope reactivity of T cells

Wild-type or HMGB1-KO clones (G9 and A10E2) of B16F10 cells (1×10^6) were s.c. injected into the flanks of B6 mice on day 0; the mice were killed on days 9 or 14, and their spleens were obtained. The spleen cells were suspended in X-vivo 15 supplemented with L-glutamine, 50 μM 2-mercaptoethanol, 50 μg/ml gentamicin, and 20 units/ml IL-2 (Shionogi) at a concentration of 5×10^6 cells/ml. One milliliter of cell suspension with 10 μg of neoepitope peptide was cultured in individual wells of a 24-well plate at 37°C in a 5% CO_2 incubator. On day 3 of culture, half the volume of the medium was replaced with fresh medium containing the peptide and IL-2. On day 6, the cells were harvested. After washing, the cells were resuspended in the medium without IL-2 and further cultured in an IFN-γ ELISPOT plate (2×10^5 cells/0.2 ml/well) in the presence or absence of the peptide (2 μg/well). After 18 h culture, IFN-γ-producing cell spots were visualized and counted by ImmunoSpot Analyzer.

2.8 | Statistical analysis

Differences between two groups were analyzed using Student's t-test. p-values < 0.05 were considered statistically significant. Statistical analyses were performed using JMP Pro version 15 software (SAS Institute).

3 | RESULTS

3.1 | Identification of CTL-epitopes of neoantigens

Whole-exosome sequencing and RNA-seq of B16F10 cells identified a total of 848 gene mutations, including 566 nonsynonymous mutations. We obtained 1207 9-mer or 10-mer peptide sequences possessing the potential for H-2K^b or H-2D^b binding. The IC50s of the binding affinity ranged from 6.29 to 39,004 nM. The IC50s of the mutated peptide sequences were compared with those of the non-mutated WT sequences:

Affinity index (AI) = IC50 of WT sequence/IC50 of mutated sequence.

We selected 602 mutated peptide sequences with AI ≥ 1 and further categorized them into three groups as follows: "fair" peptides with 5 > AI ≥ 1, "good" peptides with 10 > AI ≥ 5, and "very good" peptides with AI ≥ 10. Using this category, we obtained 525 fair, 46 good, and 31 very good peptides from the total 602 mutated peptides. After excluding several sequences with high contents (>70%) of hydrophobic residues (without acidic or basic residues) that were expected to be difficult to synthesize and solubilize in physiological buffers, 50 mutated peptide sequences with higher binding affinity (IC50 < 283 nM) to H-2K^b or H-2D^b were chosen, and custom-made synthetic peptides were obtained. The sequences and characteristics of the 50 mutated peptides are shown in Table S1.

3.2 | In vivo immunogenicity of the neoepitope peptides

Each of the 50 selected mutated peptides was s.c. injected to three mice on days 0 and 7, and the spleen cells were obtained on day 14 and subjected to IFN-γ ELISPOT assay (Figure 1A). Representative images of positive (Trp-2 and Mu19) and negative (Mu13) wells of spleen cells from peptide-immunized mice are shown in Figure 1B. Spot numbers of IFN-γ-producing cells for positive peptides are shown in Figure 1C. Each bar shows the results for an individual mouse. In the first screening, 10 peptides expressed immunogenicity under the present system while the remaining 40 peptides showed no positive responses. In the second screening, those 10 peptides were subjected to the same procedures, and the immunogenicity of all 10 peptides was confirmed. The in vivo immunogenicity of WT sequence peptides corresponding to the 10 neoepitope peptides is also shown in Figure 1C. The WT peptide (W43) corresponding to the Mu43 peptide showed a positive response. Therefore, Mu43

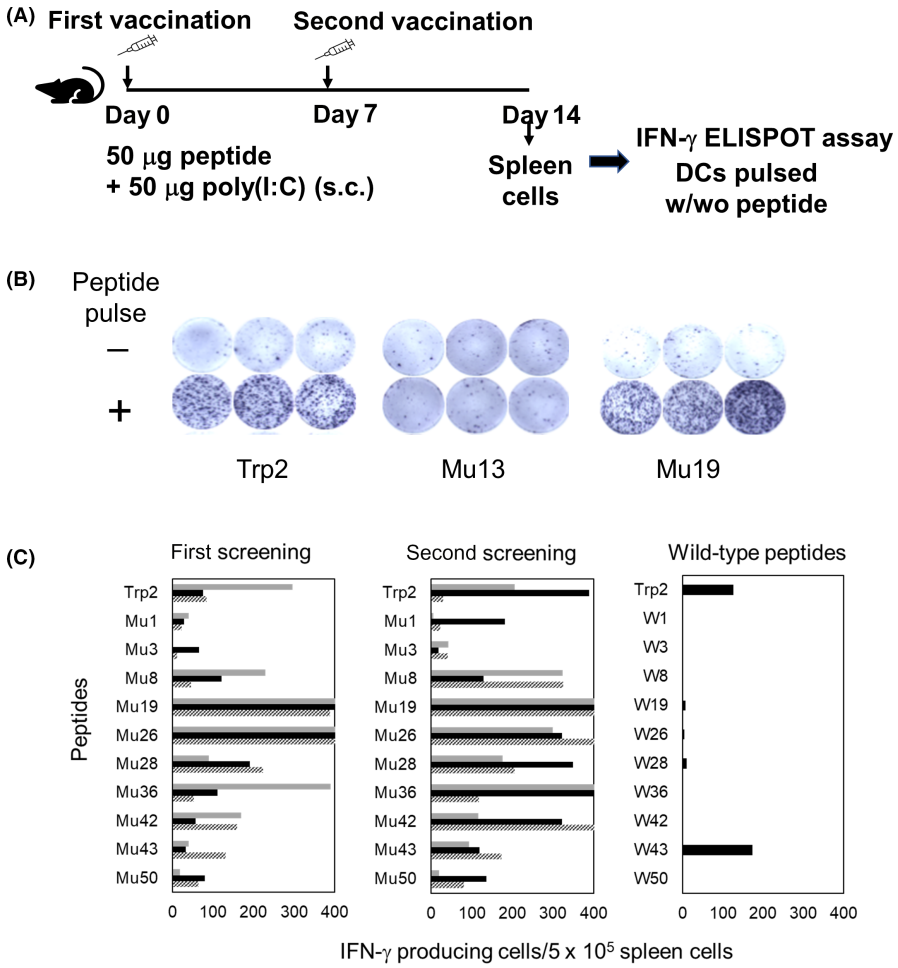

FIGURE 1 In vivo immunogenicity of the neoepitope peptides. Each of 50 mutated or control Trp-2 peptides was subcutaneously (s.c.) injected into three mice on days 0 and 7, and the spleen cells were obtained on day 14 and subjected to IFN-γ ELISPOT assay (A). Representative images of positive (Trp-2 and Mu19) and negative (Mu13) wells of spleen cells from peptide-immunized mice (B). First and second screening results of IFN-γ ELISPOT assay of positive peptides and results of wild-type peptides are also shown (C). Each bar shows the result for individual mice ($n = 3$)

was deleted from the candidates and further analyzed on the remaining nine peptides.

3.3 | Characteristics of the neoantigen peptides and genes

Characteristics of the nine immunogenic neo-epitope peptides are shown in Table 1. The expected MHC binding and amino acid lengths of the nine peptides are as follows: five H-2K^b-binding 9-mer peptides, two H-2K^b-binding 10-mer peptides, and two H-2D^b-binding 9-mer peptides. The mutated residue of each peptide is underlined with a bold letter. Anchor residues of the peptides are at position 2, 3 and the C-terminal for H-2K^b-binding and position 2, 5 and the C-terminal for H-2D^b-binding.[29] According to this rule, four peptides (Mu3, Mu28, Mu42, and Mu50) contained anchor mutation. The estimated IC50 of mutated and wild epitopes and AI are also shown in Table 1. Gene names and functions of the neoantigen-encoded genes are summarized in Table 2.

3.4 | Neoantigen reactivity of the T cells from tumor-bearing mice

We next investigated whether neoantigen-reactive T cells were present in B16F10 tumor-bearing mice. We previously established HMGB1-KO clones of B16F10 cells, and the in vivo tumor growth of these clones was reported to be markedly suppressed by CD8-mediated host immunity;[21] thus, the WT as well as the HMGB1-KO clones (G9 and A10E2) of B16F10 cells were used in the present experiment. Spleen cells were obtained from tumor-bearing mice or control non-tumor bearers on day 9; after 6 days of in vitro culture with one of the neoantigen peptides, the cells were subjected to IFN-γ ELISPOT assay (Figure 2). In vitro immunogenicity of WT peptides was also examined using spleen cells from non-tumor bearers. T cells reactive to each of the nine neoantigen peptides were detected in the spleens of WT B16F10 tumor-bearing mice. Similar T cell reactivities to the neoantigens were also detected in the HMGB1-KO clones (i.e., the G9- and A10E2-bearing mice). Basal T cell response levels to Mu26 and Mu42 as well as to Trp2 in the control non-tumor bearers were relatively higher than those to the other neoantigens; thus, the enhancing effect of tumor transplantation was less effective. Regardless, these results suggest that the nine neoantigen peptides induced CTLs in the HMGB1-KO as well as the WT B16F10 tumor-bearing mice. Spleen cells obtained on day 14 from tumor-bearing mice were also subjected to IFN-γ ELISPOT assay after 6 days of culture. The ratio of IFN-γ-producing cells in the spleens of day 9 or day 14 tumor-bearing mice to those of non-tumor controls is plotted for each peptide and shown as the "IFN-γ ELISPOT index" in Figure 3. The indexes of WT tumor-bearing mice on day 14 were increased more than twofold in Mu1, Mu3, Mu8, Mu19, Mu36, and Mu50. Such an apparent increase of the indexes was not observed in the other

TABLE 1 Characteristics of the neoantigen peptides

Mutated peptide name	Gene symbol	Nucleotide substitution	Amino acid substitution	H-2 class I allele	Length	Mutated epitope		Wild epitope		Affinity index[b]
						Sequence[a]	Ann IC50 (nM)	Sequence	Ann IC50 (nM)	
Mu1	Lins	c.461A>C	p.K154T	H-2-Db	9	RMLQNSD**T**L	6.3	RMLQNSDKL	21.2	3.37
Mu3	Alms1	c.7733A>C	p.K2578T	H-2-Kb	9	A**T**FYFHHPV	14.4	AKFYFHHPV	160.2	11.16
Mu8	Tulp2	c.1526A>C	p.K509T	H-2-Db	9	ASV**T**NFQIV	31.9	ASVKNFQIV	77.7	2.44
Mu19	Map3k6	c.952C>G	p.H318D	H-2-Kb	9	VCF**D**YTFAL	108.5	VCFHYTFAL	120.7	1.11
Mu26	Herc2	c.13349G>T	p.C4450F	H-2-Kb	10	SVFGQM**F**AKM	133.3	SVFGQMCAKM	680.0	5.10
Mu28	Actn4	c.2503T>G	p.F835V	H-2-Kb	9	VTFQAFID**V**	140.3	VTFQAFIDF	272.3	1.94
Mu36	Arvcf	c.1997G>A	p.R666H	H-2-Kb	10	EVV**H**LYLSLL	189.1	EVVRLYLSLL	242.5	1.28
Mu42	Tmem39a	c.372C>A	p.F124L	H-2-Kb	9	LIDYYLAA**L**	234.5	LIDYYLAAF	769.7	3.28
Mu50	Map1s	c.2641T>G	p.F881V	H-2-Kb	9	N**V**FLRVRAL	282.4	NFFLRVRAL	424.5	1.50

[a]The mutated residue of each peptide is underlined with a bold letter.
[b]Affinity index (AI) = IC50 of wild-type sequence/IC50 of mutated sequence.

TABLE 2 Function of neoantigen encoded genes

Mutated peptide name	Gene symbol	Gene name	GenBank accession number	Function[a]
Mu1	Lins	Lines homolog 1	NM_152815	Unknown
Mu3	Alms1	ALMS1, centrosome and basal body associated	NM_145223	Alpha-actinin binding, microtubule binding
Mu8	Tulp2	Tubby-like protein 2	NM_001045555	Phosphoric diester hydrolase activity, protein-containing complex binding
Mu19	Map3k6	Mitogen-activated protein kinase kinase kinase 6	NM_016693	MAP kinase kinase kinase activity
Mu26	Herc2	HECT and RLD domain containing E3 ubiquitin protein ligase 2	NM_010418	Transferase activity, DNA repair related
Mu28	Actn4	Actinin alpha 4	NM_021895	Transcription coactivator activity, protein homodimerization activity
Mu36	Arvcf	Armadillo repeat gene deleted in velocardiofacial syndrome	NM_001272028	Cadherin binding, protein binding, cell adhesion-related
Mu42	Tmem39a	Transmembrane protein 39a	NM_001205286	Unknown
Mu50	Map1s	Microtubule-associated protein 1S	NM_173013	DNA binding, actin filament binding, microtubule binding

[a]Functions were searched by NCBI 'Gene', https://www.ncbi.nlm.nih.gov/gene.

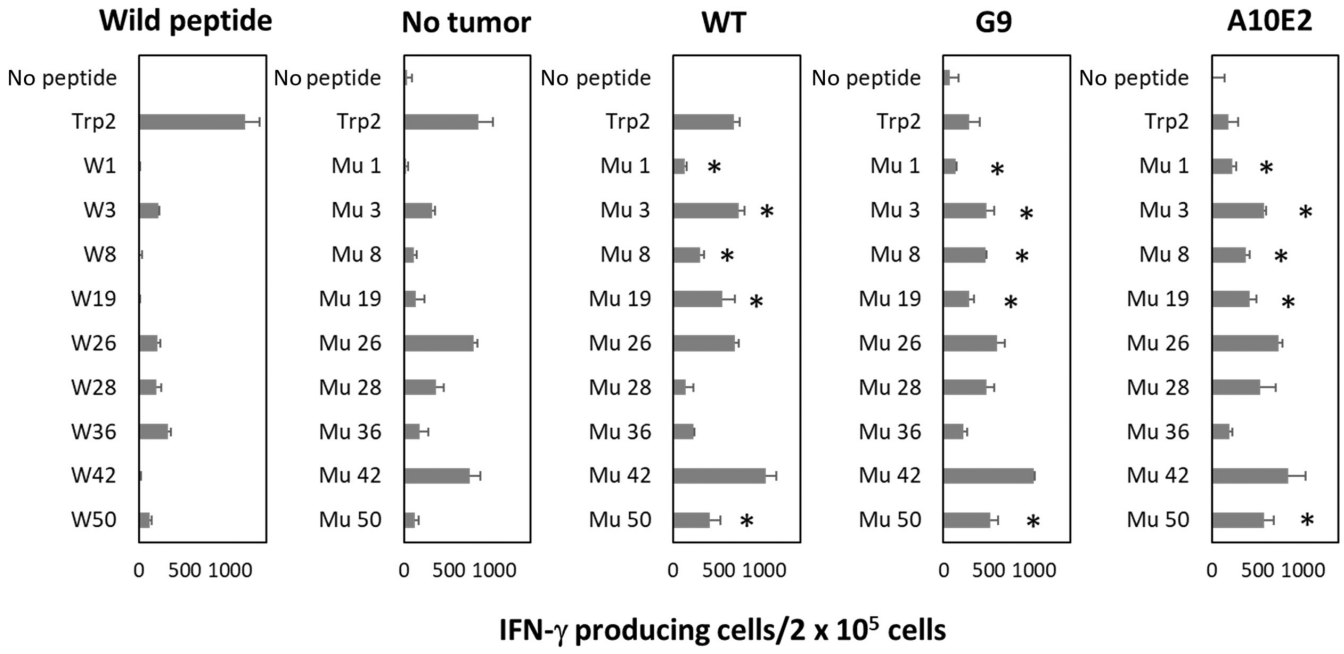

FIGURE 2 Neoantigen reactivity of T cells from tumor-bearing mice. Wild-type (WT) and two HMGB1-KO clones (G9 and A10E2) of B16F10 cells were s.c. transplanted on day 0, and spleen cells were obtained on day 9 from tumor-bearing mice or control non-tumor bearers. After 6 days in vitro culture with one of the neoantigen peptides or control Trp2 peptide, the cells were subjected to IFN-γ ELISPOT assay. In vitro immunogenicity of wild-type peptides was also examined using spleen cells from non-tumor bearers. The error bar shows the standard error of the mean. *Significantly different from no-tumor controls, $p < 0.05$

peptides. In the increased peptides, the indexes of HMGB1-KO tumor-bearers on day 9 were at roughly the same levels as those of the WT tumor-bearing mice, and the indexes of HMGB1-KO tumor-bearers in some peptides were decreased on day 14. These results might reflect the degree of antigen exposure because the size of HMGB1-KO tumors was markedly smaller than that of WT tumors on day 9 or later.

3.5 | T cell receptor repertoire of neoantigen peptide-immunized mice

The CDR3 of TcR-β in spleen cells from mice immunized with each neo-epitope peptide were analyzed. Nucleotide sequences, usage of V-, D-, and J-alleles and amino acid sequences of the CDR3 of the top 10 TcR clones of the neo-epitope peptide-immunized mice are

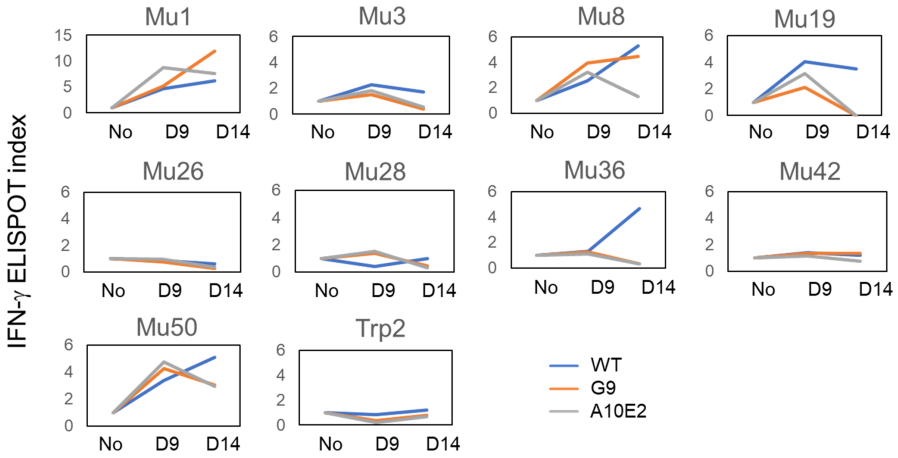

FIGURE 3 "IFN-γ ELISPOT index." The ratios of IFN-γ-producing cells in the spleens on days 9 or 14 of tumor-bearing mice to those of non-tumor controls were plotted for each peptide

TABLE 3 Neoantigen-reactive TcR clones were expanded in the wild type as well as HMGB1 knockout B16F10 tumor-bearing mice[a]

Mutated peptide name	TcR β-chain CDR3 amino acid sequence	Peptide immune[b] Spleen Frequency (%)	Non-immune[c] Spleen	WT, Day 14[d] Spleen	WT, Day 14[d] TIL	G9, Day 14[d] Spleen	G9, Day 14[d] TIL	A10E2, Day 14[d] Spleen	A10E2, Day 14[d] TIL
Mu1	CASSPTGGLSYEQYF	**0.095**	0.000	0.000	0.000	0.000	0.000	**0.029**	0.000
	CASSTGGYAEQFF	**0.051**	0.000	0.000	0.000	**0.003**	0.000	0.000	**0.005**
	CASSQEAISNERLFF	**0.047**	0.000	0.000	0.000	0.000	0.000	**0.017**	0.000
Mu3	CASSLTGGASQNTLYF	**0.151**	0.000	0.000	0.000	**0.003**	0.000	0.000	0.000
	CASSAGENTLYF	**0.068**	0.000	0.000	0.000	**0.004**	0.000	0.000	0.000
Mu8	CASSPGQISNERLFF	**0.094**	0.000	**0.014**	0.000	0.000	**0.001**	0.000	**0.003**
	CASSHRDYAEQFF	**0.057**	0.000	**0.006**	0.000	0.000	0.000	0.000	0.000
	CTCSADGANTGQLYF	**0.055**	0.000	**0.033**	0.000	0.000	0.000	0.000	0.000
Mu26	CASSQGLGGEQYF	**0.275**	0.000	0.000	0.000	0.000	0.000	0.000	**0.001**
Mu28	CASSGDRVGNTLYF	**0.162**	0.000	0.000	0.000	0.000	**0.045**	0.000	0.000
	CASSPGHNNQAPLF	**0.082**	0.000	0.000	0.000	0.000	**0.006**	0.000	0.001
Mu36	CASSLEGSQNTLYF	**0.110**	0.000	0.000	0.000	**0.003**	0.000	**0.013**	0.000
Mu42	CASSPGQNSDYTF	**0.156**	0.000	**0.022**	0.000	**0.016**	**0.006**	0.000	0.000
	CASSLTGASQNTLYF	**0.128**	0.000	0.000	0.000	0.000	0.000	**0.014**	0.000
Mu43	CASSSGTGVLEQYF	**0.135**	0.000	0.000	**0.016**	0.000	0.000	0.000	0.000
	CASSPWGSGNTLYF	**0.129**	0.000	0.000	0.000	**0.002**	0.000	0.000	0.000
	CASSPGTTNTEVFF	**0.088**	0.000	0.000	0.000	**0.006**	**0.012**	0.000	0.000
	CASSEGQGASYEQYF	**0.048**	0.000	0.000	0.000	**0.002**	0.000	0.000	0.000
Mu50	CASSQGTTYNSPLYF	**0.048**	0.000	0.000	0.000	**0.001**	0.000	0.000	0.000
	CASSLTGSSYEQYF	**0.042**	0.000	**0.010**	0.000	0.000	0.000	0.000	**0.057**
	CGARDWGSSYEQYF	**0.042**	0.000	**0.007**	0.000	**0.022**	0.000	**0.002**	0.000
Trp2	CASSLGDRGLAEQFF	**0.142**	0.000	0.000	0.000	0.000	0.000	0.000	**0.001**
	CASSLLGGRSAETLYF	**0.070**	0.000	0.000	0.000	**0.015**	0.000	0.000	0.000
	CASSPDNYEQYF	**0.069**	0.000	**0.013**	0.000	0.000	0.000	**0.001**	0.000
	CASSPGGAETLYF	**0.062**	0.000	0.000	0.000	0.000	0.000	**0.005**	0.000

[a]Frequency in the spleens and tumor-infiltrated lymphocytes (TILs) of wild-type (WT), G9, and A10E2 tumor-bearing mice of the top ~15 of abundant CDR3aa detected in the mutated peptide immunized mice was analyzed and CDR3aa detected (more than 0.001%) in any of WT, G9, or A10E2 tumor-bearing mice or non-immune mice are shown. Values more than 0.001% are shown in bold.

[b]Spleen cells from mutated or Trp2 peptide immunized mice were used for the analysis.

[c]Spleen cells from non-immune naive mice were used for the analysis.

[d]Spleen cells TILs from WT, G9. or A10E2 tumor-bearing mice were used for the analysis.

shown in Table S2. Amino acid sequences of the CDR3 of TcRmu3.1 and TcRmu3.5 were identical, although nucleotide sequences of the clones differed. Therefore, the frequency of the same CDR3 usage at amino acid levels was expected to be higher. Indeed, the CDR3 amino acid sequence of the TcRmu3.1 or TcRmu3.5 clone, "CASSLDGDTLYF," shared two more TcR clones. The number of TcR clones sharing the same CDR amino acid sequence ranges from one to eight in the 10 various neo-epitope peptide-immunized groups (Table S3).

3.6 | T cell receptor repertoire of tumor-bearing mice

The CDR3 usage at amino acid levels (CDR3aa) in the spleens and TILs of WT, G9, and A10E2 tumor-bearing mice were further analyzed. The frequencies in the spleens and TILs of WT, G9, and A10E2 tumor-bearing mice of the top ~15 most abundant CDR3aa detected in the neoantigen peptide-immunized mice were analyzed, and the CDR3aa detected (≥0.001%) in WT, G9, and A10E2 tumor-bearing mice are shown in Table 3. The number of positive (≥0.001%) CDR3aa in the spleen cells and TILs in each tumor group were as follows: 7 and 0 for WT, 8 and 4 for G9, and 7 and 5 for A10E2, respectively.

4 | DISCUSSION

We identified nine immunogenic neoantigen epitopes from 848 gene mutations, including 566 nonsynonymous mutations of B16F10 cells. Most of the gene mutations coding neoepitopes (Table S1) were included in a recent report by Lam et al.[32] as supplementary data but not in the earlier study by Castle et al.[33] These differences might be due to the progress of next-generation sequencing technology rather than to differences in the cells used since all B16F10 cells used in these three studies were obtained from ATCC. It is worth noting that for some reason, we did not detect the gene mutation encoding as promising neoantigens in the previous studies. Therefore, we did not compare the neoantigen peptides identified in the present study and the previously identified neoantigen peptides.

Four of the nine neo-epitope peptides (Mu3, Mu28, Mu42, and Mu50) contained mutations at the anchor residue for binding to H-2K^b molecules. These mutations at anchor residues caused an increase of binding affinities to the H-2K^b molecules; that is, the binding affinities of the mutants were 11.2-, 1.94-, 3.28-, and 1.50-fold higher than those of the WT peptides, respectively (Table 1). However, no apparent differences in binding affinities were observed between the anchor-residue mutation group and the nonanchor-residue mutation group of 10 peptides. Similarly, there was no difference in immunogenicity between the anchor- and nonanchor-residue mutations (Figure 1C). Preliminary results in a prophylactic vaccination model showed that some of the peptides (Mu36, Mu42) exhibited vaccination efficacy (Figure S1). These preliminary results again showed that there was no difference between the anchor- and nonanchor-residue mutations. A previous report suggested that some neoantigen peptides could function in an inhibitory manner.[32] However, our preliminary results in a prophylactic vaccination model did not show the inhibitory effects (Figure S1).

The IFN-γ ELISPOT assay demonstrated that neoantigen-reactive T cells were increased in B16F10 tumor-bearing mice. TcR repertoire analysis suggested that neoantigen-reactive T cells were oligoclonally increased in B16F10 tumor bearers. These results indicate that the nine neoantigen peptides induced CTLs in the HMGB1-KO as well as the WT B16F10 tumor-bearing mice. The ratio of IFN-γ-producing cells in WT tumor-bearing mice to IFN-γ-producing cells in the non-tumor bearers on day 14 was increased or roughly the same as that on day 9. By contrast, the ratio of IFN-γ-producing cells in HMGB1-KO tumor-bearers to IFN-γ-producing cells in the non-tumor bearers on day 14 was decreased compared to that on day 9 for most peptides. These results might reflect the amount of tumor antigens released to the TME and the subsequent exposure of the immune systems to these antigens, since the size of HMGB1-KO tumors was markedly smaller than that of WT tumors after day 9; that is, the tumor sizes of WT, G9, and A10E2 mice at day 14 were 1024 ± 391, 86 ± 19, and $278 \pm 119\,mm^3$, respectively (data not shown).

We previously suggested that suppression of tumor-derived HMGB1 might be a strategy for improving the clinical outcomes of cancer immunotherapies, including ICB and cancer vaccine therapies.[21,22] HMGB1-targeted gene editing as well as HMGB1 inhibitors are among the possible manipulation tools to suppress HMGB1 in the TME. In the present study, expansion of neoantigen-reactive T cells was observed in the WT tumor-bearing mice at both the IFN-γ ELISPOT and TcR repertoire levels, and a similar increase of neoantigen-reactive T cells was observed in the HMGB1-KO tumor-bearing mice. These results suggested that the suppression of tumor-derived HMGB1 in the TME did not inhibit the induction of neoantigen-specific immunity.

In conclusion, we identified neoantigens of B16F10 murine melanoma cells and demonstrated that suppression of HMGB1 in the TME did not inhibit the induction of neoantigen-specific immunity. These results support further development of therapies combining HMGB1 suppression with neoantigen-targeted cancer immunotherapies, including ICB therapy.

AUTHOR CONTRIBUTIONS

KW designed and performed the experiments, analyzed and validated data, and wrote, edited and reviewed the manuscript. MO performed the experiments and analyzed data. AY conceptualized and supervised the study, analyzed data, and wrote, reviewed and edited the manuscript. KW and AY confirm the authenticity of all the raw data. All authors commented previous versions of the manuscript. All authors have read and approved the final version of the manuscript.

ACKNOWLEDGMENTS

We thank Dr Osamu Ohara, Kazusa DNA Research Institute (Kisarazu, Japan), for his advice regarding next-generation sequencing analysis.

We also thank Ms Keiko Yamamoto (Kurume University) for technical assistance. This study was supported by a JSPS KAKENHI grant [no. JP19K07742 to AY].

DISCLOSURE

The authors have no conflict of interest.

ETHICS STATEMENT

Approval of the research protocol by an Institutional Reviewer Board: N/A.

Informed consent: N/A.

Registry and the registration no. Of the study/trial: N/A.

Animal Studies: All animal experimental protocols were approved by the Institutional Animal Care and Use Committee of Kurume University (approval no. 2019-030) in accordance with the national guidelines for the care and use of laboratory animals before starting the study. All gene modification experimental protocols were approved by the Institutional Genetic Modification Safety Committee of Kurume University (approval no. 30-11) in accordance with the national guidelines for research involving recombinant DNA experiments.

ORCID

Akira Yamada https://orcid.org/0000-0003-3157-9070

REFERENCES

1. Snyder A, Makarov V, Merghoub T, et al. Genetic basis for clinical response to CTLA-4 blockade in melanoma. *N Engl J Med*. 2014;371(23):2189-2199. doi:10.1056/NEJMoa1406498
2. Schumacher TN, Schreiber RD. Neoantigens in cancer immunotherapy. *Science*. 2015;348(6230):69-74. doi:10.1126/science.aaa4971
3. Goodman AM, Kato S, Bazhenova L, et al. Tumor mutational burden as an independent predictor of response to immunotherapy in diverse cancers. *Mol Cancer Ther*. 2017;16(11):2598-2608. doi:10.1158/1535-7163
4. Samstein RM, Lee CH, Shoushtari AN, et al. Tumor mutational load predicts survival after immunotherapy across multiple cancer types. *Nat Genet*. 2019;51(2):202-206. doi:10.1038/s41588-018-0312-8
5. Turajlic S, Litchfield K, Xu H, et al. Insertion-and-deletion-derived tumourspecific neoantigens and the immunogenic phenotype: a pan-cancer analysis. *Lancet Oncol*. 2017;18(8):1009-1021. doi:10.1016/S1470-2045(17)30516-8
6. Patel SA, Minn AJ. Combination cancer therapy with immune checkpoint blockade: mechanisms and strategies. *Immunity*. 2018;48(3):417-433. doi:10.1016/j.immuni.2018.03.007
7. Galon J, Bruni D. Approaches to treat immune hot, altered and cold tumours with combination immunotherapies. *Nat Rev Drug Discov*. 2019;18(3):197-218. doi:10.1038/s41573-018-0007-y
8. Galluzzi L, Humeau J, Buqué A, Zitvogel L, Kroemer G. Immunostimulation with chemotherapy in the era of immune checkpoint inhibitors. *Nat Rev Clin Oncol*. 2020;17(12):725-741. doi:10.1038/s41571-020-0413-z
9. Yamada A, Sasada T, Noguchi M, Itoh K. Next-generation peptide vaccines for advanced cancer. *Cancer Sci*. 2013;104(1):15-21. doi:10.1111/cas.12050
10. Sasada T, Yamada A, Noguchi M, Itoh K. Personalized peptide vaccine for treatment of advanced cancer. *Curr Med Chem*. 2014;21(21):2332-2345. doi:10.2174/09298673216614020513293
11. Sakamoto S, Noguchi M, Yamada A, Itoh K, Sasada T. Prospect and progress of personalized peptide vaccinations for advanced cancers. *Expert Opin Biol Ther*. 2016;16(5):689-698. doi:10.1517/14712598.2016.1161752
12. Cheever MA, Allison JP, Ferris AS, et al. The prioritization of cancer antigens: a national cancer institute pilot project for the acceleration of translational research. *Clin Cancer Res*. 2009;15(17):5323-5337. doi:10.1158/1078-0432.CCR-09-0737
13. Butterfield LH. Cancer vaccines. *BMJ*. 2015;350:h988. doi:10.1136/bmj.h988
14. Carreno BM, Magrini V, Becker-Hapak M, et al. Cancer immunotherapy. A dendritic cell vaccine increases the breadth and diversity of melanoma neoantigen-specific T cells. *Science*. 2015;348(6236):803-808. doi:10.1126/science.aaa3828
15. Ott PA, Hu Z, Keskin DB, et al. An immunogenic personal neoantigen vaccine for patients with melanoma. *Nature*. 2017;547(7662):217-221. doi:10.1038/nature22991
16. Keskin DB, Anandappa AJ, Sun J, et al. Neoantigen vaccine generates intratumoral T cell responses in phase Ib glioblastoma trial. *Nature*. 2019;565(7738):234-239. doi:10.1038/s41586-018-0792-9
17. Kloor M, Reuschenbach M, Pauligk C, et al. A frameshift peptide neoantigen-based vaccine for mismatch repair-deficient cancers: a phase I/IIa clinical trial. *Clin Cancer Res*. 2020;26(17):4503-4510. doi:10.1158/1078-0432.CCR-19-3517
18. Ott PA, Hu-Lieskovan S, Chmielowski B, et al. A phase Ib trial of personalized neoantigen therapy plus anti-PD-1 in patients with advanced melanoma, non-small cell lung cancer, or bladder cancer. *Cell*. 2020;183(2):347-362.e24. doi:10.1016/j.cell.2020.08.053
19. Tang D, Kang R, Zeh HJ 3rd, Lotze MT. High-mobility group box 1 and cancer. *Biochim Biophys Acta*. 2010;1799(1–2):131-140. doi:10.1016/j.bbagrm.2009.11.014
20. Krysko DV, Garg AD, Kaczmarek A, Krysko O, Agostinis P, Vandenabeele P. Immunogenic cell death and DAMPs in cancer therapy. *Nat Rev Cancer*. 2012;12(12):860-875. doi:10.1038/nrc3380
21. Yokomizo K, Waki K, Ozawa M, et al. Knockout of high-mobility group box 1 in B16F10 melanoma cells induced host immunity-mediated suppression of in vivo tumor growth. *Med Oncol*. 2022;39(5):58. doi:10.1007/s12032-022-01659-2
22. Waki K, Yamada A. Blockade of high mobility group box 1 augments antitumor T-cell response induced by peptide vaccination as a co-adjuvant. *Cancer Sci*. 2016;107(12):1721-1729. doi:10.1111/cas.13084
23. Liu Z, Falo LD Jr, You Z. Knockdown of HMGB1 in tumor cells attenuates their ability to induce regulatory T cells and uncovers naturally acquired CD8 T cell-dependent antitumor immunity. *J Immunol*. 2011;187(1):118-125. doi:10.4049/jimmunol.1003378
24. Zhang Y, Liu Z, Hao X, et al. Tumor-derived high-mobility group box 1 and thymic stromal lymphopoietin are involved in modulating dendritic cells to activate T regulatory cells in a mouse model. *Cancer Immunol Immunother*. 2018;67(3):353-366. doi:10.1007/s00125-020-05105-8
25. Hubert P, Roncarati P, Demoulin S, et al. Extracellular HMGB1 blockade inhibits tumor growth through profoundly remodeling immune microenvironment and enhances checkpoint inhibitor-based immunotherapy. *J Immunother Cancer*. 2021;9(3):e001966. doi:10.1136/jitc-2020-001966
26. Kang R, Zhang Q, Zeh HJ 3rd, Lotze MT, Tang D. HMGB1 in cancer: good, bad, or both? *Clin Cancer Res*. 2013;19(15):4046-4057. doi:10.1158/1078-0432.CCR-13-0495
27. Kawai T, Akira S. Toll-like receptors and their crosstalk with other innate receptors in infection and immunity. *Immunity*. 2011;34(5):637-650. doi:10.1016/j.immuni.2011.05.006
28. Kang R, Chen R, Zhang Q, et al. HMGB1 in health and disease. *Mol Aspects Med*. 2014;40:1-116. doi:10.1016/j.mam.2014.05.001

29. Immune Epitope Database (IEDB) MHC-I binding predictions. Accessed April 21, 2022. http://tools.immuneepitope.org/mhci/
30. Schreurs MW, Eggert AA, de Boer AJ, et al. Dendritic cells break tolerance and induce protective immunity against a melanocyte differentiation antigen in an autologous melanoma model. *Cancer Res*. 2000;60(24):6995-7001.
31. Lutz MB, Suri RM, Niimi M, et al. Immature dendritic cells generated with low doses of GM-CSF in the absence of IL-4 are maturation resistant and prolong allograft survival in vivo. *Eur J Immunol*. 2000;30(7):1813-1822. doi:10.1002/1521-4141(200007)30:7%3C1813::AID-IMMU1813%3E3.0.CO;2-8
32. Lam H, McNeil LK, Starobinets H, et al. An empirical antigen selection method identifies neoantigens that either elicit broad antitumor T-cell responses or drive tumor growth. *Cancer Discov*. 2021;11(3):696-713. doi:10.1158/2159-8290.CD-20-0377
33. Castle JC, Kreiter S, Diekmann J, et al. Exploiting the mutanome for tumor vaccination. *Cancer Res*. 2012;72(5):1081-1091. doi:10.1158/0008-5472.CAN-11-3722

SUPPORTING INFORMATION

Additional supporting information can be found online in the Supporting Information section at the end of this article.

How to cite this article: Waki K, Ozawa M, Yamada A. Suppression of high mobility group box 1 in B16F10 tumor does not inhibit the induction of neoantigen-specific T cells. *Cancer Sci*. 2022;113:4082-4091. doi: 10.1111/cas.15563